The Journal of Chemical Physics ARTICLE pubs.aip.org/aip/jcp

Photolysis of the peptide bond at 193 and 222 nm

Cite as: J. Chem. Phys. 162, 165104 (2025); doi: 10.1063/5.0257551
Submitted: 10 January 2025 • Accepted: 8 April 2025 •
Published Online: 25 April 2025

View Online Export Citation CrossMark

Nicholas Drachman,[1,2] Jacob Vietorisz,[1] Andrew J. Winchester,[2] Robert Vest,[2] Gregory A. Cooksey,[2] Sujitra Pookpanratana,[2] and Derek Stein[1,a)]

AFFILIATIONS

[1] Department of Physics, Brown University, Providence, Rhode Island 02912, USA
[2] Physical Measurement Laboratory, National Institute of Standards and Technology, Gaithersburg, Maryland 20899, USA

[a)] **Author to whom correspondence should be addressed:** Derek_Stein@brown.edu

ABSTRACT

Ultraviolet (UV) light is a well-established tool for fragmenting peptides in vacuum. This study investigates the fragmentation of peptides using 193 and 222 nm light in aqueous solution. Changes in the absorption spectra of solutions of the model dipeptide glycylglycine are monitored using a combination of real-time *in situ* transmission measurements and UV–Vis spectroscopy to report peptide bond scission following UV irradiation. Irradiation by a broadband ultraviolet light source flattens the absorbance peak centered near 193 nm, indicating cleavage of peptide bonds. Irradiation with low-intensity, monochromatic 193 and 222 nm light enabled measurements of the single-photon quantum yield of peptide bond scission, found to be $(1.50 \pm 0.12)\%$ at 193 nm and $(0.16 \pm 0.03)\%$ at 222 nm. These findings indicate that peptides may be fragmented in solution prior to emission into a mass spectrometer for new types of single-molecule analyses. The susceptibility of peptide bonds to ultraviolet radiation also suggests limited lifetimes for peptides on the early Earth's surface, which are relevant to theories of the origins-of-life, and suggests a role for protein damage in explanations of the germicidal effect of 222 nm light exposure.

© 2025 Author(s). All article content, except where otherwise noted, is licensed under a Creative Commons Attribution-NonCommercial 4.0 International (CC BY-NC) license (https://creativecommons.org/licenses/by-nc/4.0/). https://doi.org/10.1063/5.0257551

I. INTRODUCTION

Light is widely used to fragment peptides in mass spectrometry-based proteomics.[1–8] Ultraviolet photodissociation (UVPD) is a technique that stands out for its ability to achieve extensive fragmentation and high sequence coverage, making it a powerful tool for top-down proteomics.[3,9,10] In a typical UVPD workflow, ionized proteins or peptides are irradiated by a UV laser pulse while held in an ion trap.[3] To maximize signal and sequence coverage, each ion should undergo just one fragmentation event,[3,11] generating an informative pair of N- and C-terminal fragments. Multiple fragmentations of a single precursor generate internal fragments, which complicate the analysis and are typically ignored, reducing the total usable signal.[11–13] Thousands or more copies of the protein or peptide ion of interest typically need to be fragmented to generate a sufficiently detailed fragmentation spectrum to identify the ion.[14] The need for large ensembles of precursor ions makes these UVPD methods fundamentally unsuitable for single-molecule analyses. The aim of analyzing and sequencing single protein molecules has received growing interest, driven by the need to provide ultimate sensitivity for detecting low-abundance proteins and enabling comprehensive single-cell proteomics,[15–18] but UVPD methods have not yet been applied to the study of single molecules.

We envision analyzing a single peptide by fragmenting it with light in the liquid phase before every fragment is ionized and delivered into a mass spectrometer.[16,19,20] Single-molecule protein sequencing may be possible if one can preserve the ordering of fragments[21] and faithfully measure every ion. One important element of this strategy is an ion source that delivers ions with minimal loss. We have recently reported such an ion source, which uses a nanopore to deliver amino acid and small peptide ions directly into the high vacuum region of a mass spectrometer and transmit them to the detector with near unit efficiency.[20] We also theoretically analyzed the conditions required to preserve the ordering of fragments as they emerge from such a source.[21] A second element of our strategy is a method for using light to cleave peptides into separate amino acids within the ion source. This concept reverses the order of fragmentation and ionization relative to conventional UVPD. We seek to develop a suitable fragmentation method. Our first step is to identify wavelengths that efficiently induce peptide bond scission in water

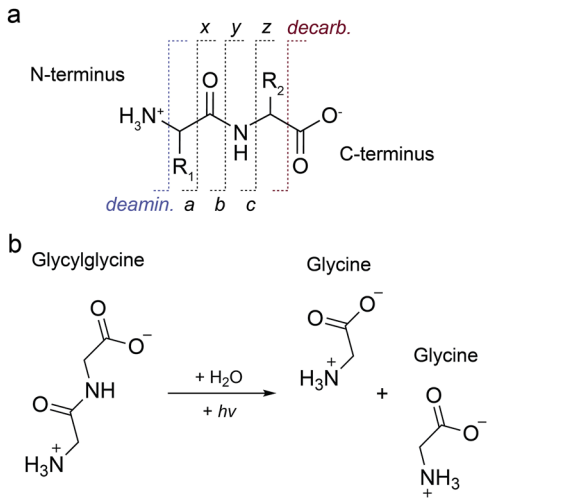


FIG. 1. (a) Standard peptide fragmentation nomenclature shown for a generic dipeptide. The deamination and decarboxylation processes are also indicated at the N- and C-termini, respectively. (b) Reaction scheme for the UV photolysis of Gly-Gly causing peptide bond scission.

and quantify the quantum yields of these processes. Ultraviolet (UV) light with a wavelength near 200 nm appears to be the ideal candidate because it is strongly absorbed by peptide bonds,[3] it carries enough energy in a single photon to break the peptide bond,[22] and it is weakly absorbed by water and quartz.[23,24]

UVPD of peptides in the gas phase has been extensively studied, particularly at 157 nm,[25–27] 193 nm,[28–30] 213 nm,[31,32] and 266 nm.[33,34] In this wavelength range, UVPD proceeds via a combination of direct dissociation pathways and internal conversion,[11] producing a diverse array of fragments. Figure 1(a) shows the standard nomenclature for peptide fragment pairs. Longer UV wavelengths (>220 nm) have been found to produce the highest fraction of b- and y-type fragments, which result from the cleavage of the peptide bond. With decreasing wavelength (and hence increasing photon energy), one obtains more a- and x-type fragments, which result from the cleavage of the backbone C–C_α bond, as well as more v- and w-type fragments from side chain cleavages.[3,27,35] This is consistent with results from collision induced dissociation (CID) experiments, where b- and y-type fragments are generated at lower energies than other fragments.[35] Near-UV photons with wavelengths of 351 and 355 nm carry less energy than the dissociation energy of the peptide bond,[22] but these wavelengths have found use in identifying post-translational modifications (PTMs), such as phosphorylation and nitration,[36,37] and in fragmenting specific peptides tagged with near-UV chromophores.[4,38]

UV fragmentation of peptides in water (termed photolysis) occurs in a complex chemical environment, making the analysis of photoproducts more challenging compared to gas-phase studies where mass spectrometry can directly measure the fragmentation products. Investigations by Nikogosyan *et al.* in the 1990s determined the molar absorption coefficients and quantum yields of scission and decomposition for a wide range of amino acids and di- and tri-peptides at several wavelengths around 200 nm.[39–43] They found that the peptide bonds were broken with quantum yields ranging from ~1% to 5%.[39,40] Around the same time, Hill *et al.* carried out detailed analyses of the photolysis products generated by the irradiation of a few dipeptides with 254 nm light and determined that deamination and decarboxylation [labeled deamin. and decarb. in Fig. 1(a)] were the primary fragmentation pathways.[44,45] More recent work by Thøgersen *et al.*[46] used UV pump–IR probe transient absorption spectroscopy to observe the photolysis of Gly-Gly over 200 ps following absorption of 200 nm photons and observed CO_2 as the only major photoproduct, which is consistent with a decarboxylation process and no cleavage of the peptide bond. Thøgersen *et al.* concluded that the peptide bonds were "unharmed by deep UV excitation";[46] however, that finding appears to be in disagreement with the earlier reports by Nikogosyan and Gorner.[40]

Here, we report measurements of the UV photolysis of Gly-Gly in aqueous solution upon irradiation by broad spectrum UV light, as well as monochromatic 193 and 222 nm light. This work seeks to clarify the question of whether single UV photons near 200 nm can break peptide bonds in aqueous solution, as illustrated in Fig. 1(b), and to establish whether this is a viable approach for our single-molecule peptide analysis scheme. Our approach combines *in situ* UV absorption measurements at the irradiation wavelength with UV–Vis spectra sampled following varying irradiation doses. Gly-Gly was chosen as a model peptide for these measurements as it is the simplest dipeptide, and the peptide bond is the only major absorber of deep UV light in the molecule. Light with a wavelength of 193 nm was chosen because it is located near the peptide bond absorbance peak and is the most common wavelength used in UVPD.[3,47] Light with a wavelength of 222 nm was also investigated because it has become widely and cost-effectively available in the form of KrCl excimer lamps following the COVID-19 pandemic due to its use in disinfection;[48–50] however, the quantum yield of peptide bond scission at 222 nm has not been previously reported. A simple model of absorption and bond scission allows us to extract the quantum yield of peptide bond scission at 193 and 222 nm from the *in situ* transmission and offline UV–Vis measurements. In addition, we discuss the relevance of these results for our single-molecule protein sequencing scheme, as well as to other fields such as origins of life and UV disinfection.

II. METHODS

A. UV absorbance measurements

Glycine and Gly-Gly were purchased in powder form (>99 % purity). Solutions were prepared by serial dilution in 18.2 MΩ cm deionized (DI) water. UV–Vis spectra down to 190 nm were obtained using a UV–Vis spectrophotometer capable of measuring liquid samples as small as 1 μl. For each measurement, a 5 μl sample droplet was pipetted onto the instrument's sample pedestal. The pedestal was rinsed three times with DI water between measurements. The instrument automatically adjusts its path length between 0.03 and 1 mm to maintain an optimal signal-to-noise ratio across a wide range of concentrations. All absorbance values in this work are reported as the equivalent absorbance for a standard 10 mm path length cuvette to enable direct comparison between measurements. We measured the UV absorption spectra of aqueous solutions of glycine and Gly-Gly to determine their respective molar

© Author(s) 2025

absorption coefficients. The solutions consisted of mixtures with linearly varying concentrations, ranging from 1 mmol l^{-1} Gly-Gly and 0 mmol l^{-1} glycine to 0 mmol l^{-1} Gly-Gly and 2 mmol l^{-1} glycine. This measurement simulates the results of an "ideal" Gly-Gly photolysis experiment, where 100% of the peptide bonds are broken, but all other bonds remain intact.

B. Broad spectrum irradiation

A laser driven light source produces broad spectrum radiation from 170 to 2500 nm using a focused laser to ignite xenon plasma. The light source has a radiance of about 10 mW mm^{-2} nm^{-1} sr^{-1} over its full wavelength range. A refocusing system consisting of two off-axis parabolic mirrors focused the output of the light source into a 0.5 × 1.0 cm^2 spot with a focal distance of about 23 cm. The light source irradiated 0.25 ml of 5 mmol l^{-1} Gly-Gly in DI water for 90 h at an ambient temperature of about 20 C. The UV–Vis absorption spectrum of the sample was measured before and after irradiation using the UV-spectrophotometer. The volume of the sample was measured before and after irradiation to correct the spectra for increased concentration due to water evaporation.

C. 193 nm irradiation

Figure 4(a) shows our setup for irradiating and monitoring the scission of peptide bonds by 193 nm laser light *in situ*. A Ti:sapphire laser was used to generate tunable IR light in 140 fs pulses at an 80 MHz repetition rate with a total output power of around 3.5 W. The IR beam is directed through a Faraday isolator to prevent back reflections and then into a commercial harmonics module, which generates the fourth harmonic (4ω) of the fundamental frequency (ω) by utilizing ($3\omega + 1\omega$) mixing. We tuned the IR laser to 772 nm so that the harmonics module would output a 193 nm beam. The power is significantly reduced with each harmonic generated, resulting in a typical output power of around 0.5 mW at 193 nm and a beam radius of about 0.5 mm. The UV beam is directed into an acrylic enclosure that is continuously purged with N_2 to remove oxygen, which absorbs strongly at 193 nm. The beam passes through an aperture and is then directed toward a beam splitter using two UV mirrors. The splitter directs about 20% of the beam toward a reference powermeter to track the laser power, which may drift over the duration of an experiment. The remainder of the beam passes through a 1 cm path length quartz cuvette containing the sample solution and then strikes the sample powermeter. The sample is continuously stirred with a magnetic stir bar, which is kept near the edge of the cuvette to avoid interfering with the beam. A second powermeter measures the transmission of 193 nm light through the sample.

D. 222 nm irradiation

A 222 nm KrCl excimer lamp irradiated samples inside of a light-tight box. The box contained the UV lamp, a 1 cm path length quartz cuvette containing the sample solution, a photodiode designed for 222 nm measurements, cooling fans, a custom circuit to process the photodiode signal and power the device, and an opaque separator with a 1 × 3 cm^2 window to direct the UV light toward the cuvette and prevent stray light from damaging the circuit. The cooling fans provide sufficient cooling power to ensure that the temperature of the sample solution does not change appreciably over the course of irradiation. The signal processing circuit consisted of a transimpedance amplifier with a gain of 10^7 to convert the small photodiode current into an easily measurable voltage, as well as a first-order low pass filter (10 kΩ, 1 μF) to smooth out the lamp's rapid discharges.

We irradiated 3 ml of 1 mmol l^{-1} Gly-Gly in DI water for 63 h at an ambient temperature of about 20 °C. The transmitted power was continuously measured throughout the entire duration of the experiment. The sample cuvette was periodically replaced with an identical cuvette containing 3 ml of pure DI water in order to track drift in the incident power, allowing us to calculate the transmission and absorbance according to $T = I_T/I_I = 10^{-A}$, where T is the transmission, I_T is the transmitted light intensity, I_I is the incident light intensity, and A is the absorbance. We periodically withdrew 50 μl aliquots of the sample solution using a micropipette and froze them for later UV–Vis measurements.

E. Uncertainty analysis

The measurements in this study have three primary sources of uncertainty: (1) instrument reproducibility in measuring a single solution, (2) sample preparation reproducibility including pipetting and weighing uncertainties, and (3) process reproducibility of the photolysis experiments. For absorption coefficient measurements, we quantified sources (1) and (2) by performing three repeated measurements of each solution and by preparing four independent mixtures of Gly-Gly and glycine solutions. The dominant uncertainty came from sample preparation using micropipettes with ~10% uncertainty (one standard error). For quantum yield determinations, we fit our experimental data to a kinetic model that takes the measured absorption coefficients as input parameters. To account for how uncertainties in these input parameters affect the fitted quantum yields, we performed Monte Carlo simulations sampled from the uncertainty distributions of both the initial concentrations and the measured absorption coefficients. All uncertainties are reported as one standard error unless otherwise specified.

III. RESULTS AND DISCUSSION

A. UV absorbance of glycine, Gly-Gly, and the peptide bond

Figure 2(a) shows the UV absorption spectra of five aqueous mixtures with different concentrations of Gly-Gly and glycine. The concentrations were varied such that the total number of glycine moieties is conserved as the ratio of Gly-Gly to glycine changes. All absorbance values are given as the equivalent absorbance for a 10 mm path length. The absorbance at $\lambda < 210$ nm increases approximately linearly with increasing Gly-Gly concentration, suggesting that the peptide bond is the dominant chromophore in this wavelength range. Figure 2(b) shows that the absorbance at 193 nm, A_{193}, increases approximately linearly with Gly-Gly concentration c_{GG}. This indicates that A_{193} is a good measure of the peptide bond concentration. Comparing A_{193} at $c_{GG} = 0$ mmol l^{-1} and 1 mmol l^{-1}, we find that a peptide bond absorbs 193 nm light 27 ± 1 times more strongly than a glycine moiety, where the uncertainty is given as the standard deviation of three repeated measurements.

© Author(s) 2025

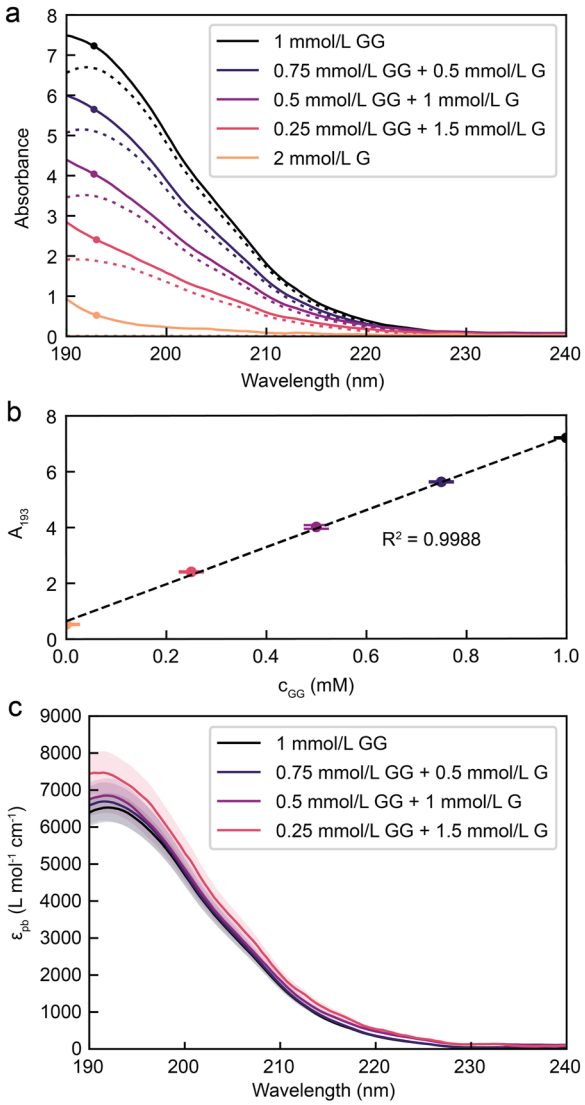


FIG. 2. (a) Absorption spectra of aqueous mixtures of Gly-Gly (GG) and glycine (G). Each curve represents the mean of three repeated measurements. The dashed curves show the absorption spectrum of each mixture after subtracting the absorbance of 2 mmol l^{-1} glycine. The dots correspond to the absorbance at 193 nm, A_{193}. (b) Plot A_{193} vs Gly-Gly concentration along with a linear fit. Error bars correspond to the standard deviation of three repeated measurements. (c) The molar absorption coefficient of the peptide bond, ε_{pb}, as a function of wavelength for each mixture of Gly-Gly and glycine.

We obtain the molar absorption coefficients at a particular wavelength, λ, of Gly-Gly and glycine from the absorbance spectra of 1 mmol l^{-1} Gly-Gly and 2 mmol l^{-1} glycine, respectively, using the Beer–Lambert law,

$$A_\lambda = \varepsilon_\lambda c l, \tag{1}$$

where A_λ and ε_λ are the absorbance and molar absorption coefficients, respectively, and l is the path length. The absorption cross section σ_λ (in units of cm^2) is obtained from the molar absorption coefficient (measured in mol^{-1} L cm^{-1}) using

$$\sigma = \frac{10^3 \ln(10)}{N_A}\varepsilon, \tag{2}$$

where N_A is Avogadro's number. Table I shows the measured ε_λ and σ_λ values for glycine and Gly-Gly at λ = 193 and 222 nm.

TABLE I. Molar absorption coefficients and absorption cross sections for glycine and Gly-Gly. All ε values have units of M^{-1} cm^{-1} and σ values have units of cm^2. Each value has a relative uncertainty (one standard error) of ~10%, primarily due to the concentration uncertainty.

	ε_{193}	σ_{193}	ε_{222}	σ_{222}
Glycine	265	1.01×10^{-18}	15	5.74×10^{-20}
Gly-Gly	7200	2.75×10^{-17}	280	1.07×10^{-18}

We calculated the molar absorption coefficient of the peptide bond, $\varepsilon_{pb,\lambda}$, by first subtracting the absorbance of 2 mmol l^{-1} glycine from the absorbance of the other mixtures to isolate the contribution from the peptide bond [dashed spectra in Fig. 2(a)] and then using Eq. (1) to obtain $\varepsilon_{pb,\lambda}$ from A_λ. Figure 2(c) shows four independent measurements of $\varepsilon_{pb,\lambda}$ obtained from the four different mixtures containing Gly-Gly. The four independent measurements agree within the experimental uncertainty. The estimate of ε_{pb} decreases slightly with increasing Gly-Gly concentration, a trend that may be explained by an underestimation of the Gly-Gly stock solution concentration. The uncertainty in ε_{pb} is due primarily to uncertainty in the concentration of the stock solutions and diluted mixtures, as these were prepared with a 10 μl micropipette, which has close to 10 % uncertainty (one standard error). At 193 nm, we measure $\varepsilon_{pb} = (6700 \pm 600)$ mol^{-1} L cm^{-1}, where the uncertainty again corresponds to one standard error, in agreement with a previous measurement by Mulcahy *et al.*[39]

The peak in ε_{pb} around λ = 193 nm indicates that this is the optimal wavelength with which to *monitor* the photolysis of Gly-Gly; this wavelength offers the highest sensitivity to changes in peptide concentration due to bond scission. However, this does not necessarily imply that 193 nm is the optimal wavelength for *specifically fragmenting* the peptide bond.

B. Broad spectrum irradiation

We turn now to the possibility of breaking peptide bonds in solution with UV light. As a first test of feasibility, we irradiated a 5 mmol l^{-1} aqueous Gly-Gly solution with a broad-spectrum light source (170–2500 nm; ≈25 mW mm^{-2} sr nm) for 90 h to see if any fragmentation would occur and produce a measurable change in the absorption spectrum. We measured the UV–Vis absorption spectrum before and after irradiation, and each measurement was repeated five times to estimate the uncertainty. The absorption spectrum of the irradiated Gly-Gly solution was corrected for the evaporation of solvent by measuring the volume before and after irradiation and scaling the concentration accordingly.

Figure 3 shows the change in the UV absorbance spectrum for 5 mmol l^{-1} Gly-Gly. After 90 h of irradiation, the absorbance at 193 nm fell by a factor of about 15. Figure 3 also shows the UV–Vis

© Author(s) 2025

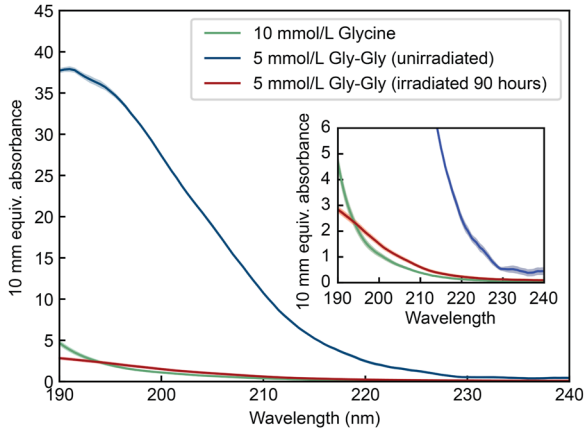


FIG. 3. UV absorption spectrum of 5 mmol l^{-1} aqueous Gly-Gly before and after 90 h of irradiation with a broad spectrum light source. The measured spectrum of unirradiated 10 mmol l^{-1} glycine is also shown for comparison. Shaded areas (similar in thickness to the solid lines) represent the standard deviation of repeated measurements. The inset shows the same plot with a smaller y-range, providing a more detailed view of the irradiated Gly-Gly and unirradiated glycine spectra.

spectrum of a 10 mmol l^{-1} aqueous solution of glycine to compare the irradiated spectrum with the "ideal" spectrum, which would result if all peptide bonds were broken, forming two glycines for every Gly-Gly, with no other light-induced chemical changes. The glycine spectrum is very similar to that of the irradiated Gly-Gly, suggesting that the majority of peptide bonds holding together the dipeptides were broken. This result is interesting in and of itself, as it demonstrates that the peptide bond is, indeed, fragmented following irradiation by a broad spectrum UV light source. However, we cannot draw any conclusions about which wavelength is primarily responsible for the bond scission from this experiment alone, due to the broad spectrum emission of the light source.

C. 193 nm irradiation

We turn our attention to monochromatic UV irradiation, beginning with 193 nm light. Light with $\lambda = 193$ nm is near the absorption peak of the peptide bond and is commonly used in UVPD, so this wavelength is a good candidate for peptide photolysis. In addition, the quantum yield of scission of Gly-Gly at 193 nm has been previously reported by Nikogosyan *et al.* (albeit measured by a somewhat different technique), providing a point of comparison for our results.[39]

We measured the photolysis of Gly-Gly under low intensity, 193 nm laser irradiation. 193 nm laser light separately irradiated an aqueous solution of 100 μmol l^{-1} Gly-Gly and an aqueous solution of 200 μmol l^{-1} glycine, both at pH 6.5, at an average power of 370 μW for 1 h each at an ambient temperature of about 20 °C. Due to the low laser power, the total energy deposited in the solution over the course of irradiation is insufficient to appreciably change its temperature. The transmission was measured continuously *in situ*. Every 10 min, the top of the purged enclosure was opened for ~10–20 s and a small aliquot of solution was drawn from the cuvette using a micropipette to measure the full UV–Vis in a separate spectrophotometer. Figure 4(b) shows the evolution of the

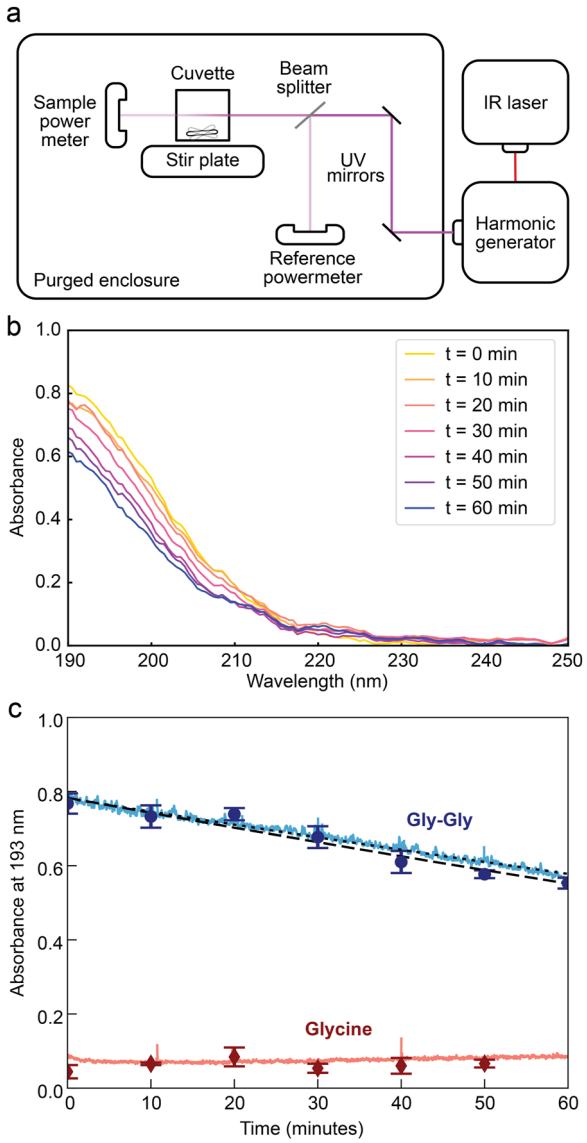


FIG. 4. (a) Schematic of the 193 nm irradiation and monitoring experiment. (b) UV–Vis spectra of 200 μmol l^{-1} Gly-Gly solutions at pH 6.5 collected at 10 min intervals during irradiation with 193 nm pulsed laser light. (c) Absorbance of Gly-Gly (blue) and glycine (red) at 193 nm measured both *in situ* during irradiation (lighter solid lines) and from the UV–Vis spectrum (circles). The error bars represent the standard error of three repeated measurements. The quantum yield of scission is determined from the fits to both Gly-Gly measurements (black dotted line for *in situ* and black dashed line for UV–Vis).

UV absorption spectrum of 100 μM Gly-Gly (pH 6.5) over 1 h of irradiation with 193 nm pulsed laser light. There is an ~30% decrease in absorbance at 193 nm. Figure 4(c) plots the measured absorbance at 193 nm from both the *in situ* transmission measurement and the UV–Vis spectra as a function of irradiation time. The plot additionally shows the separate control measurement of the absorbance at

© Author(s) 2025

193 nm of a 200 μmol l^{-1} solution of glycine. Both the *in situ* transmission and offline UV–Vis methods yield similar results and agree that the absorbance of Gly-Gly at 193 nm falls by about 30% over 1 h of 193 nm irradiation, while the glycine sample's absorbance remains unchanged.

These observations indicate that the decrease in absorbance with irradiation must be due to the cleavage of the peptide bond rather than other photochemical modifications of the glycine moieties. The constant absorbance of the glycine control sample demonstrates that any UV-induced chemical changes to the amino acid portions of Gly-Gly cannot account for the observed spectral changes, as these would have also affected the absorbance of the glycine solution.

The quantum yield of peptide bond scission, Φ_λ, is the ratio of peptide bonds broken to the number of absorbed photons of wavelength λ. We find Φ_λ by fitting a kinetic model of photolysis to the measured absorbance at 193 nm. The kinetic model (derived in Appendix A) relates the changing concentrations of Gly-Gly and glycine to the absorbance at 193 nm via the molar absorption coefficients ($\varepsilon_{i,193}, i = \mathrm{GG}, \mathrm{G}$), the sample geometry (i.e., the irradiated cross-sectional area A_c, sample volume V, and path length l), the incident power density I_0, photon energy E_v, and the quantum yield Φ_λ,

$$\frac{dc_{\mathrm{GG}}}{dt} = -\frac{A_c I_0}{10^3 V N_A E_v}\Phi_\lambda\left(1 - 10^{-A_\lambda(t)}\right), \tag{3}$$

where N_A is Avogadro's number and A_λ is the absorbance at the irradiation wavelength λ,

$$A_\lambda(t) = \varepsilon_{\mathrm{GG},\lambda} c_{\mathrm{GG}}(t) l + \varepsilon_{\mathrm{G},\lambda} c_{\mathrm{G}}(t) l. \tag{4}$$

The kinetic model yields predictions for $A_{193}(t)$ that depend on the free parameters $\varepsilon_{\mathrm{GG},193}$ and Φ_{193}. $\varepsilon_{\mathrm{G},193}$ is constrained by the measured ratio of $\varepsilon_{\mathrm{GG},193}/\varepsilon_{\mathrm{G},193}$ from Sec. III A.

The fit to the *in situ* measurement yields $\Phi_{193} = (1.44 \pm 0.16)\%$ and $\varepsilon_{\mathrm{GG},193} = (7810 \pm 820)$ L mol^{-1} cm^{-1}, and the UV–Vis measurement gives $\Phi_{193} = (1.57 \pm 0.18)\%$ and $\varepsilon_{\mathrm{GG},193} = (7830 \pm 820)$ L mol^{-1} cm^{-1}. Uncertainties in the fitted parameters (corresponding to one standard error) were determined through Monte Carlo simulations that account for the uncertainty in initial solution concentrations and uncertainties in the measured molar absorbance coefficients. These two independent measurements agree within the experimental uncertainty, giving a mean Φ_{193} value of 1.50% with a root-mean-square uncertainty of 0.12%. The best fit $\varepsilon_{\mathrm{GG},193}$ values agree with those measured by Nikogosyan *et al.*, while the Φ_{193} value is lower than that reported by Nikogosyan *et al.* by about 40%.[39] In that work, Φ_{193} was determined by measuring absorbance at 210 nm at only two time-points, before and after irradiation. In contrast, we determined the quantum yield of peptide bond scission by two independent time-series measurements of the absorbance at 193 nm, a far more sensitive wavelength for measuring the presence of peptide bonds.

UVPD is believed to fragment peptides along two independent pathways:[3,11,51] In the direct dissociation pathway, the absorbed photon promotes a binding electron into a dissociative orbital, which leads immediately to bond scission. The internal conversion pathway, by contrast, involves the absorbed photon's energy being redistributed among vibrational modes before causing bond scission at a random site. We hypothesize that the quantum yield will be lower in solution than in vacuum due to rapid transfer of thermal energy from an excited peptide to the surrounding water, suppressing the internal conversion dissociation pathway. Unfortunately, a direct comparison is not yet possible because the quantum yield of peptide bond scission *in vacuo* at 193 nm has not been reported. An estimate of the photodissociation cross section, σ_{pd}, based upon the best available data still cannot support our hypothesis. The published results and experimental parameters from Brodbelt *et al.*[52,53] reveal that a 1 mJ pulse results in the fragmentation of about 30% of precursor myoglobin ions. We assume that the pulse is uniformly distributed over a 15 mm^2 spot size[54] as no focusing optics are mentioned.[52,53] These values result in an estimated photodissociation cross section of $\sigma_{pd} \approx 5 \times 10^{-17}$ cm^2. To compare this with our measurements in aqueous solution, we first determine σ_{pd} for Gly-Gly by taking the product of the *absorption* cross section and the quantum yield of peptide bond scission. This value is then multiplied by the number of peptide bonds in myoglobin, 153, yielding $\sigma_{pd} \approx 7 \times 10^{-17}$ cm^2. The similarity of these two values does not provide any evidence that dissociation processes that are allowed in vacuum are suppressed in solution.

D. 222 nm irradiation

We next investigated the photolysis of Gly-Gly upon irradiation by 222 nm light. A 222 nm (5.6 eV) photon carries less energy than a 193 nm photon (6.4 eV), so it may be expected to have a lower quantum yield of bond scission as the reduced excess energy can be more easily dissipated by the molecule and surrounding solvent. At the same time, the lower energy of 222 nm photons may result in more specific peptide bond cleavage rather than inducing other chemical changes. It is additionally important to investigate the effect of 222 nm irradiation on peptides as this wavelength has found widespread use in disinfection lamps following the COVID-19 pandemic.

Figure 5(a) shows a schematic of the experiment in which 222 nm light irradiates samples. A 222 nm KrCl excimer lamp irradiated 3 ml of aqueous 1 mmol l^{-1} Gly-Gly (pH 6.5) at an irradiance of about 3.5 mW cm^{-2} while periodically withdrawing and freezing 50 μl samples for offline UV–Vis spectroscopy. Figure 5(b) shows the evolution of the UV absorption spectrum of the Gly-Gly solution over 63 h of irradiation. The spectra show a monotonic decrease in absorbance between 190 and 220 nm upon irradiation, similar to the changes seen upon irradiation with 193 nm light. It is interesting to note that at the irradiation wavelength of 222 nm, the absorbance has a more complex behavior, as shown in Fig. 5(c). The non-monotonicity may be due to other chemical changes besides peptide bond scission. 222 nm absorbance is, therefore, a poor choice for *monitoring* peptide fragmentation.

Because we measured the full UV–Vis spectrum at multiple times during irradiation, we can extract the absorbance at 193 nm vs time [like in Fig. 4(c)] despite this not being the irradiation wavelength. Figure 5(d) plots the measured absorbance at 193 nm from the UV–Vis spectra as a function of time. The monotonic decrease in absorbance at 193 nm provides clear evidence for the progressive loss of peptide bonds during irradiation, in contrast to the complex

© Author(s) 2025

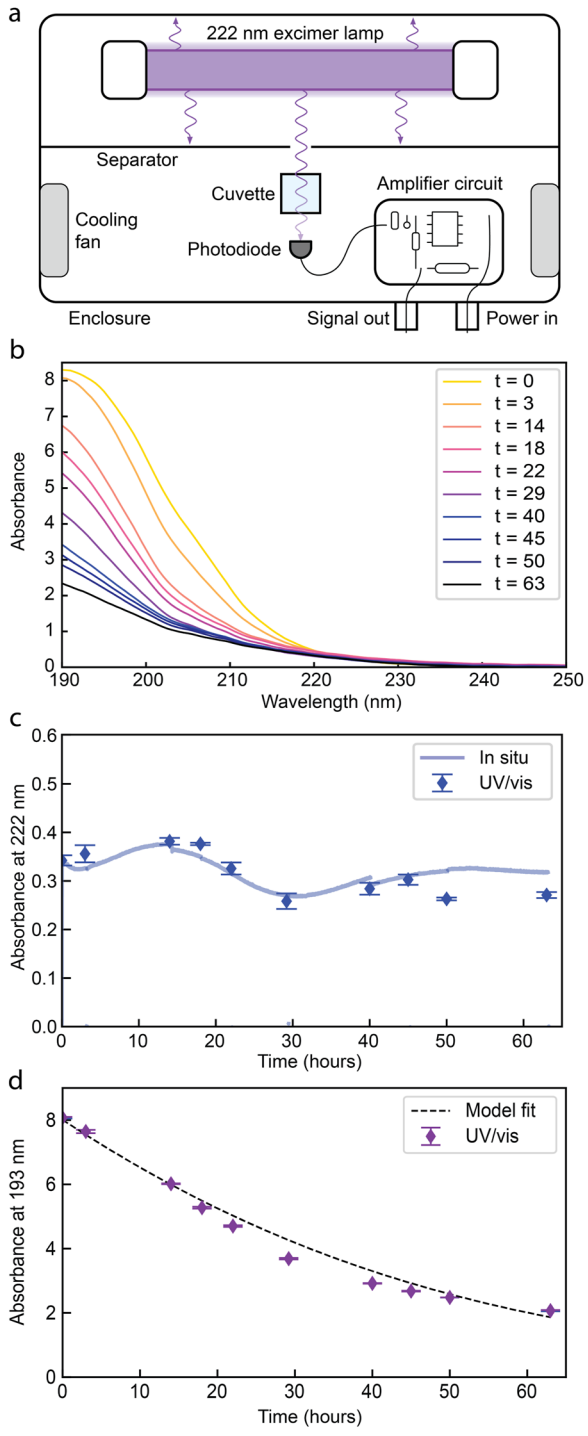


FIG. 5. (a) Schematic of 222 nm irradiation and monitoring experiment. (b) UV spectra of 1 mmol l^{-1} Gly-Gly at pH 6.5 collected following various durations (in hours) of irradiation with 222 nm light. (c) Absorbance of Gly-Gly at 222 nm from both the *in situ* and UV–Vis measurements. (d) Absorbance of Gly-Gly at 193 nm from the UV–Vis measurements and the model fit used to find the quantum yield. Error bars correspond to standard deviations of three repeated measurements.

fluctuating behavior observed at 222 nm. By the end of the experiment, the 193 nm absorbance has decreased by ~40%, indicating substantial peptide bond cleavage.

The quantum yield of peptide bond scission at 222 nm, Φ_{222}, is determined using the same fitting approach described in Sec. III C, applying Eqs. (3) and (4) with $\lambda = 222$ nm. The free parameters are again $\varepsilon_{GG,193}$ and Φ_{222}, with all other molar absorption coefficients ($\varepsilon_{G,193}$, $\varepsilon_{G,222}$, and $\varepsilon_{GG,222}$) constrained by their ratios to $\varepsilon_{GG,193}$, measured in Sec. III A. The fit yields $\Phi_{222} = 0.16\% \pm 0.03\%$ for 222 nm irradiation, where the uncertainty is again determined through Monte Carlo simulations that account for the uncertainty in initial solution concentrations and uncertainties in the measured molar absorbance coefficients. Φ_{222} is ~1 order of magnitude smaller than the Φ_{193} value found in Sec. III C. Despite the low quantum yield of scission, these results still demonstrate unambiguously that peptide bonds can be broken in solution by 222 nm light.

E. Implications for single-molecule peptide sequencing

Knowledge of the quantum yield of peptide bond scission allows us to estimate the experimental requirements to efficiently fragment peptides for single-molecule analysis. The measured quantum yield values are summarized in Table II. Combining the absorption and scission processes yields the average photodissociation rate for a particular species, $J\sigma_\lambda\Phi_\lambda$, where J is the photon flux (m^{-2} s^{-1}) and σ_λ is the absorption cross section at the irradiation wavelength λ (m^2). The cumulative probability that a particular peptide bond has been broken following t seconds of irradiation is then given by

$$P(t) = 1 - e^{-J\sigma_\lambda\Phi_\lambda t}. \quad (5)$$

Figure 6 shows a plot of $P(t)$ for four different incident power densities at 193 nm [Fig. 6(a)] and 222 nm [Fig. 6(b)]. The plots were generated using the $\Phi_{sc,\lambda}$ and ε_λ values summarized in Tables I and II. We find that 193 nm light can break peptide bonds more than two orders of magnitude faster than 222 nm light at the same incident power density. This is due to its 25-fold higher absorption coefficient and 10-fold higher quantum yield of peptide bond scission. Commercially available 193 nm ArF excimer lasers, which are widely used in UVPD experiments, can reach time-averaged power densities on the order of 10^5 W m^{-2} to 10^6 W m^{-2}, so efficient cleavage of peptides within the ion source should be achievable on a timescale of tens of milliseconds.[53–55] 193 nm is a better choice of wavelength if high throughput is desired, as it breaks peptide bonds with markedly higher efficiency than 222 nm. In addition, 222 nm light sources tend to have lower power densities.[56,57]

TABLE II. Measured quantum yield of peptide bond scission for Gly-Gly at 193 and 222 nm. Φ_{193} is presented as the mean of the *in situ* and UV–Vis measurements ± the combined uncertainty (one standard error) of the two measurements.

	Φ_{193} (%)	Φ_{222} (%)
Gly-Gly	1.50 ± 0.12	0.16 ± 0.03

© Author(s) 2025

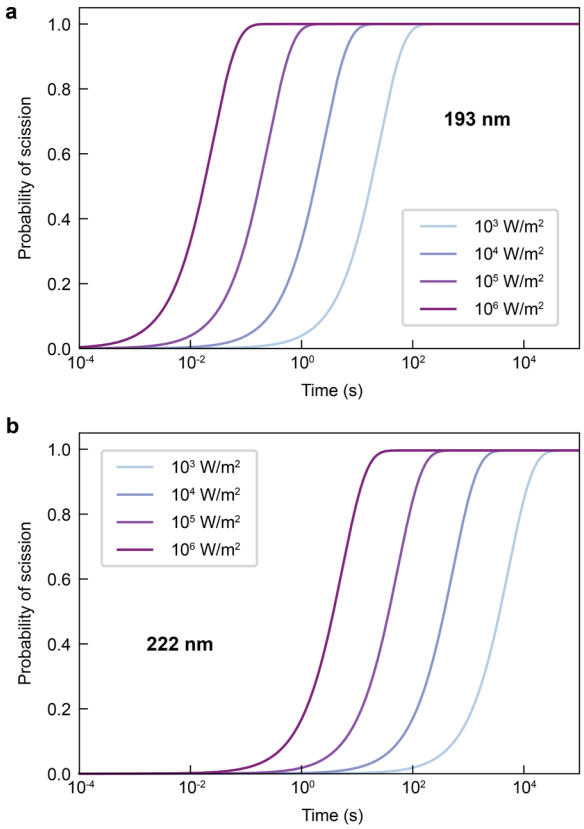


FIG. 6. Power requirements for peptide bond scission at (a) 193 nm and (b) 222 nm.

F. Broader implications

The susceptibility of the peptide bond to UV photolysis has broader implications for fields such as origins-of-life and UV disinfection. For the first life to develop, the organic molecules involved in prebiotic chemistry had to persist long enough to interact and form more complex structures. The UV photolysis of the peptide bond limits the expected lifetime of small peptides under early Earth conditions. Models of the solar photon flux incident at Earth's surface 3.9×10^9 years ago indicate that $\sim 10^{13}$ photons in the wavelength range of 200–230 nm would strike each square centimeter of the Earth's surface each second.[58] Lower wavelengths would have been effectively screened by atmospheric H_2O and CO_2. Prebiotic freshwater bodies were largely transparent to UV with wavelengths longer than 200 nm.[59] Using Eq. (5) and an estimated quantum yield of 0.1% to 1% for this wavelength range, we estimate that the lifetime of a peptide bond on the surface of the early Earth is on the order of 10^6 s, or several days. This is far faster than the uncatalyzed hydrolysis of peptides, which occurs on a timescale of hundreds of years.[60] The UV-induced degradation of peptides appears to be underappreciated in the origin-of-life field, as it goes unmentioned in major reviews of prebiotic peptide chemistry.[61,62]

In addition, the application of 222 nm UV light in disinfection processes should carefully consider the potential for protein damage. Studies of the germicidal effect of 222 nm irradiation typically focus on damage to nucleic acids,[50,63] and proteins are typically thought to provide protection by absorbing the light before it reaches the DNA in the nucleus.[48,49,63,64] Damage to those same proteins is typically not considered in great detail and may warrant further consideration in future studies of the germicidal properties and human safety profile of 222 nm light.

IV. CONCLUSIONS

This study has demonstrated the feasibility of using ultraviolet (UV) light at 193 and 222 nm to induce peptide bond scission in aqueous solutions. Through a combination of *in situ* transmission measurements and offline UV–Vis spectroscopy, we have shown that Gly-Gly can be fragmented by UV light, with single photon quantum yields of ~1.5% at 193 nm and 0.16% at 222 nm. These findings support the feasibility of our single-molecule protein sequencing approach. In addition, power considerations favor the use of 193 nm over 222 nm to ensure rapid efficient bond cleavage. Future work that combines UV photolysis with mass spectrometry could shed additional light on the specific photochemical pathways involved and the products generated. Ensuring that amino acid side chains remain largely intact while peptide bonds are cleaved will be essential for integrating UV photolysis into a mass spectrometry workflow for single-molecule peptide analysis.

ACKNOWLEDGMENTS

N.D. and D.S. thank Dr. Amit Agarwal, who first introduced us to Dr. Pookpanratana, making this collaboration possible. A.J.W. was supported by the NRC Postdoctoral Associateship program. J.V. was supported by Brown University's Undergraduate Teaching and Research Awards program. N.D. was supported by the Graduate Fellowships for STEM Diversity, Oxford Nanopore Technologies, and the NHGRI of the National Institutes of Health under Award No. R21HG021938.

AUTHOR DECLARATIONS

Conflict of Interest

D.S., N.D., and J.V. are listed as inventors on patents and patent applications that are licensed to Oxford Nanopore Technologies, Plc., in which they declare a financial interest.

Author Contributions

N.D. led the research design, data collection, and manuscript preparation. J.V. contributed to the 222 nm irradiation research design and data collection. A.J.W. and S.P. designed and built the experimental setup used for the 193 nm irradiation experiments and helped with data collection. R.V. contributed to the research design and data collection for the broad spectrum irradiation experiments. G.A.C. contributed to the research design and helped acquire funding. D.S. conceived and supervised the project and helped acquire funding.

© Author(s) 2025

Nicholas Drachman: Conceptualization (equal); Formal analysis (equal); Investigation (equal); Methodology (equal); Software (equal); Writing – original draft (equal); Writing – review & editing (equal). **Jacob Vietorisz**: Formal analysis (supporting); Investigation (supporting); Methodology (supporting); Writing – review & editing (supporting). **Andrew J. Winchester**: Investigation (supporting); Methodology (supporting); Resources (supporting); Writing – review & editing (supporting). **Robert Vest**: Investigation (supporting); Methodology (supporting); Resources (supporting). **Gregory A. Cooksey**: Project administration (equal); Resources (supporting); Supervision (equal); Writing – review & editing (supporting). **Sujitra Pookpanratana**: Methodology (equal); Project administration (supporting); Resources (equal); Supervision (supporting); Writing – review & editing (supporting). **Derek Stein**: Conceptualization (equal); Formal analysis (supporting); Funding acquisition (lead); Methodology (equal); Project administration (equal); Resources (supporting); Supervision (lead); Writing – original draft (supporting); Writing – review & editing (lead).

DATA AVAILABILITY

The data that support the findings of this study are available from the corresponding author upon reasonable request.

APPENDIX A: MODEL OF PHOTOFRAGMENTATION

We developed a simple physical model that describes the rate of peptide bond scission as a function of the irradiance, peptide concentration, molar absorption coefficient, and the geometry of the irradiation setup. We begin by defining the absorbed light intensity, $I_{abs} = I_0 - I$, where I_0 is the incident intensity and I is the transmitted intensity, both having units of W m^{-2}. Using Beer's law, we find that

$$I_{abs} = I_0\left(1 - 10^{-\varepsilon_\lambda c l}\right), \tag{A1}$$

where c is the peptide concentration, ε_λ is the molar absorption coefficient at the wavelength of the incident light, and l is the path length through the sample. The absorbed intensity is related to the number of absorbed photons, N_{abs}, by

$$dN_{abs} = I_{abs} A_c dt / E_v, \tag{A2}$$

where dt is the total irradiation time, A_c is the illuminated cross-sectional area of the sample (not to be confused with the absorption cross section), and E_v is the photon energy. We then find the change in peptide concentration resulting from peptide bond scission, Δc, by multiplying N_{abs} by the quantum yield of peptide bond scission, Φ_λ, and applying the necessary unit conversions,

$$dc = -\frac{dN_{abs}}{10^3 V N_A}\Phi_\lambda \tag{A3}$$

$$= -\frac{A I_0}{10^3 V N_A E_v}\Phi_\lambda\left(1 - 10^{-\varepsilon_\lambda c l}\right)dt. \tag{A4}$$

Avogadro's number, N_A, and the volume, V, appear in Eq. (A4) to convert the total number to concentration, while the factor of 10^3 converts the units from mol m^{-3} to mol L^{-1}. This can then be rewritten as an ordinary differential equation (ODE), which can be solved numerically,

$$\frac{dc}{dt} = -\frac{A_c I_0}{10^3 V N_A E_v}\Phi_\lambda\left(1 - 10^{-\varepsilon_\lambda c(t) l}\right). \tag{A5}$$

For 193 nm irradiation experiments, we monitor the absorbance at 193 nm over time, $A_{193}(t)$, which is related to the concentrations of Gly-Gly (c_{GG}) and glycine (c_G) by

$$A_{193}(t) = \varepsilon_{GG,193} c_{GG}(t) l + \varepsilon_{G,193} c_G(t) l, \tag{A6}$$

where $c_{GG}(t)$ and $c_G(t)$ are determined by solving the coupled differential equations,

$$\frac{dc_{GG}}{dt} = -\frac{A_c I_0}{10^3 V N_A E_v}\Phi_{193}\left(1 - 10^{-A_{193}(t)}\right), \tag{A7}$$

$$\frac{dc_G}{dt} = -2\frac{dc_{GG}}{dt}. \tag{A8}$$

For 222 nm irradiation experiments, we still monitor the absorbance at 193 nm over time but use the absorbance at 222 nm, the irradiation wavelength, to determine the change in concentration. The absorbance at 222 nm is given by

$$A_{222}(t) = \varepsilon_{GG,222} c_{GG}(t) l + \varepsilon_{G,222} c_G(t) l, \tag{A9}$$

where the concentrations are determined by solving

$$\frac{dc_{GG}}{dt} = -\frac{A_c I_0}{10^3 V N_A E_v}\Phi_{222}\left(1 - 10^{-A_{222}(t)}\right) \tag{A10}$$

and Eq. (A8).

For both wavelengths, experimental measurements of $A_{193}(t)$ are fit to Eq. (A6), where $c_{GG}(t)$ and $c_G(t)$ are determined by numerically integrating Eqs. (A7) and (A8) in the case of 193 nm irradiation, or Eqs. (A8) and (A10) in the case of 222 nm irradiation.

APPENDIX B: MULTIPHOTON ABSORPTION IN 193 nm EXPERIMENTS

To accurately measure the absorption coefficient and quantum yield, it is important to avoid multiphoton processes that would confound the measurements. By multiphoton process, we specifically mean the absorption of additional photons by a single molecule before it has time to relax or break after an initial photon absorption. The timescale for the internal conversion of an excited molecule in solution is on the order of 10^{-14} to 10^{-11} s,[65,66] so we want to ensure that the time between photon absorption events for a single molecule is significantly longer than this. Given that the laser repetition frequency is 80 MHz with a pulse width of 140 fs, there is a gap of about 12.5 ns between laser pulses, much longer than the timescale of electron relaxation. So, we only need to consider the probability of absorbing multiple photons during a single laser pulse.

The probability that any molecule absorbs one photon during a laser pulse, P_1, can be simply approximated by the ratio of the number of absorbed photons during one pulse, N_{abs}, to the number of Gly-Gly molecules in the beam path, N_{GG},

$$P_1 \approx \frac{N_{abs}}{N_{GG}}. \tag{B1}$$

© Author(s) 2025

The number of Gly-Gly molecules in the beam path is the product of the concentration and the volume of the beam path with appropriate unit conversions,

$$N_{GG} = 10^3 N_A cl(\pi r_{beam}^2). \quad \text{(B2)}$$

To find N_{abs}, we first divide the laser power, P, by the frequency, f, and the energy per photon to get the number of photons in a pulse and then multiply by the fraction of photons absorbed,

$$N_{abs} = \frac{P}{fE_v}(1 - 10^{-\varepsilon cl}). \quad \text{(B3)}$$

Plugging the values $c = 1$ mmol l^{-1}, $P = 0.5$ mW, $f = 80$ MHz, $r_{beam} = 0.5$ mm, $l = 1$ cm, and $\varepsilon = 7200$ mol^{-1} l cm^{-1} into Eq. (B1), we find that any given molecule has a probability of just about 10^{-8} of absorbing a photon during a single laser pulse. We can, therefore, conclude that the probability of a single molecule absorbing multiple photons during a single pulse is very small and unlikely to have any effect on the measurement. A similar calculation for the 222 nm irradiation conditions reveals an even lower probability of multi-photon absorption processes in those experiments.

REFERENCES

[1] J. S. Brodbelt, "Photodissociation mass spectrometry: New tools for characterization of biological molecules," Chem. Soc. Rev. **43**, 2757–2783 (2014).
[2] J. S. Brodbelt, "Ion activation methods for peptides and proteins," Anal. Chem. **88**, 30–51 (2016).
[3] J. S. Brodbelt, L. J. Morrison, and I. Santos, "Ultraviolet photodissociation mass spectrometry for analysis of biological molecules," Chem. Rev. **120**, 3328–3380 (2019).
[4] J. J. Wilson and J. S. Brodbelt, "MS/MS simplification by 355 nm ultraviolet photodissociation of chromophore-derivatized peptides in a quadrupole ion trap," Anal. Chem. **79**, 7883–7892 (2007).
[5] C.-K. Lai, D. C. M. Ng, H. F. Pang, J. C. Y. Le Blanc, J. W. Hager, D.-C. Fang, A. S.-C. Cheung, and I. K. Chu, "Laser-induced dissociation of singly protonated peptides at 193 and 266 nm within a hybrid linear ion trap mass spectrometer," Rapid Commun. Mass Spectrom. **27**, 1119–1127 (2013).
[6] K. L. Fort, A. Dyachenko, C. M. Potel, E. Corradini, F. Marino, A. Barendregt, A. A. Makarov, R. A. Scheltema, and A. J. R. Heck, "Implementation of ultraviolet photodissociation on a benchtop Q exactive mass spectrometer and its application to phosphoproteomics," Anal. Chem. **88**, 2303–2310 (2016).
[7] S. Dörner, L. Schwob, K. Atak, K. Schubert, R. Boll, T. Schlathölter, M. Timm, C. Bülow, V. Zamudio-Bayer, B. von Issendorff *et al.*, "Probing structural information of gas-phase peptides by near-edge X-ray absorption mass spectrometry," J. Am. Soc. Mass Spectrom. **32**, 670–684 (2021).
[8] P. Maitre, D. Scuderi, D. Corinti, B. Chiavarino, M. E. Crestoni, and S. Fornarini, "Applications of infrared multiple photon dissociation (IRMPD) to the detection of posttranslational modifications," Chem. Rev. **120**, 3261–3295 (2019).
[9] J. B. Shaw, W. Li, D. D. Holden, Y. Zhang, J. Griep-Raming, R. T. Fellers, B. P. Early, P. M. Thomas, N. L. Kelleher, and J. S. Brodbelt, "Complete protein characterization using top-down mass spectrometry and ultraviolet photodissociation," J. Am. Chem. Soc. **135**, 12646–12651 (2013).
[10] L. Fornelli, K. Srzentić, T. K. Toby, P. F. Doubleday, R. Huguet, C. Mullen, R. D. Melani, H. dos Santos Seckler, C. J. DeHart, C. R. Weisbrod *et al.*, "Thorough performance evaluation of 213 nm ultraviolet photodissociation for top-down proteomics," Mol. Cell. Proteomics **19**, 405–420 (2020).
[11] R. R. Julian, "The mechanism behind top-down UVPD experiments: Making sense of apparent contradictions," J. Am. Soc. Mass Spectrom. **28**, 1823–1826 (2017).
[12] Y. A. Lyon, D. Riggs, L. Fornelli, P. D. Compton, and R. R. Julian, "The ups and downs of repeated cleavage and internal fragment production in top-down proteomics," J. Am. Soc. Mass Spectrom. **29**, 150–157 (2017).
[13] S. D. Dunham, B. Wei, C. Lantz, J. A. Loo, and J. S. Brodbelt, "Impact of internal fragments on top-down analysis of intact proteins by 193 nm UVPD," J. Proteome Res. **22**, 170–181 (2022).
[14] D. D. Holden and J. S. Brodbelt, "Improving performance metrics of ultraviolet photodissociation mass spectrometry by selective precursor ejection," Anal. Chem. **89**, 837–846 (2017).
[15] L. Restrepo-Pérez, C. Joo, and C. Dekker, "Paving the way to single-molecule protein sequencing," Nat. Nanotechnol. **13**, 786–796 (2018).
[16] J. A. Alfaro, P. Bohländer, M. Dai, M. Filius, C. J. Howard, X. F. Van Kooten, S. Ohayon, A. Pomorski, S. Schmid, A. Aksimentiev *et al.*, "The emerging landscape of single-molecule protein sequencing technologies," Nat. Methods **18**, 604–617 (2021).
[17] B. M. Floyd and E. M. Marcotte, "Protein sequencing, one molecule at a time," Annu. Rev. Biophys. **51**, 181–200 (2022).
[18] J. Swaminathan, A. A. Boulgakov, and E. M. Marcotte, "A theoretical justification for single molecule peptide sequencing," PLoS Comput. Biol. **11**, e1004080 (2015).
[19] J. Bush, W. Maulbetsch, M. Lepoitevin, B. Wiener, M. Mihovilovic Skanata, W. Moon, C. Pruitt, and D. Stein, "The nanopore mass spectrometer," Rev. Sci. Instrum. **88**, 113307 (2017).
[20] N. Drachman, M. Lepoitevin, H. Szapary *et al.*, "Nanopore ion sources deliver individual ions of amino acids and peptides directly into high vacuum," Nat. Commun. **15**, 7709 (2024).
[21] W. Maulbetsch, B. Wiener, W. Poole, J. Bush, and D. Stein, "Preserving the sequence of a biopolymer's monomers as they enter an electrospray mass spectrometer," Phys. Rev. Appl. **6**, 054006 (2016).
[22] I. I. Marochkin and O. V. Dorofeeva, "Amide bond dissociation enthalpies: Effect of substitution on N–C bond strength," Comput. Theor. Chem. **991**, 182–191 (2012).
[23] P. T. Staveteig and J. T. Walsh, "Dynamic 193-nm optical properties of water," Appl. Opt. **35**, 3392–3403 (1996).
[24] L. A. Moore and C. M. Smith, "Fused silica as an optical material [Invited]," Opt. Mater. Express **12**, 3043–3059 (2022).
[25] Y. M. E. Fung, F. Kjeldsen, O. A. Silivra, T. W. D. Chan, and R. A. Zubarev, "Facile disulfide bond cleavage in gaseous peptide and protein cations by ultraviolet photodissociation at 157 nm," Angew. Chem., Int. Ed. **44**, 6399 (2005).
[26] F. Kjeldsen, O. A. Silivra, and R. A. Zubarev, "Zwitterionic states in gas-phase polypeptide ions revealed by 157-nm ultra-violet photodissociation," Chem. Eur. J. **12**, 7920–7928 (2006).
[27] J. P. Reilly, "Ultraviolet photofragmentation of biomolecular ions," Mass Spectrom. Rev. **28**, 425–447 (2009).
[28] D. C. Barbacci and D. H. Russell, "Sequence and side-chain specific photofragment (193 nm) ions from protonated substance P by matrix-assisted laser desorption ionization time-of-flight mass spectrometry," J. Am. Soc. Mass Spectrom. **10**, 1038–1040 (1999).
[29] M. S. Thompson, W. Cui, and J. P. Reilly, "Factors that impact the vacuum ultraviolet photofragmentation of peptide ions," J. Am. Soc. Mass Spectrom. **18**, 1439–1452 (2007).
[30] J. A. Madsen, D. R. Boutz, and J. S. Brodbelt, "Ultrafast ultraviolet photodissociation at 193 nm and its applicability to proteomic workflows," J. Proteome Res. **9**, 4205–4214 (2010).
[31] M. A. Halim, M. Girod, L. MacAleese, J. Lemoine, R. Antoine, and P. Dugourd, "213 nm ultraviolet photodissociation on peptide anions: Radical-directed fragmentation patterns," J. Am. Soc. Mass Spectrom. **27**, 474–486 (2015).
[32] S. Becher, H. Wang, M. G. Leeming, W. A. Donald, and S. Heiles, "Influence of protein ion charge state on 213 nm top-down UVPD," Analyst **146**, 3977–3987 (2021).
[33] S. Becher, B. Spengler, and S. Heiles, "Effects of wavelength, fluence, and dose on fragmentation pathways and photoproduct ion yield in 213 nm and 266 nm ultraviolet photodissociation experiments," Eur. J. Mass Spectrom. **24**, 54–65 (2018).

© Author(s) 2025

[34] A. Agarwal, J. K. Diedrich, and R. R. Julian, "Direct elucidation of disulfide bond partners using ultraviolet photodissociation mass spectrometry," Anal. Chem. **83**, 6455–6458 (2011).
[35] J. S. Klassen and P. Kebarle, "Collision-induced dissociation threshold energies of protonated glycine, glycinamide, and some related small peptides and peptide amino amides," J. Am. Chem. Soc. **119**, 6552–6563 (1997).
[36] C. J. Shaffer, K. Slováková, and F. Tureček, "Near-UV photodissociation of phosphopeptide cation-radicals," Int. J. Mass Spectrom. **390**, 71–80 (2015).
[37] Y. S. Shin, J. H. Moon, and M. S. Kim, "Selective screening of tyrosine-nitrated peptides in tryptic mixtures by in-source photodissociation at 355 nm in matrix-assisted laser desorption ionization," Anal. Chem. **83**, 1704–1708 (2011).
[38] J. R. Aponte, L. Vasicek, J. Swaminathan, H. Xu, M. C. Koag, S. Lee, and J. S. Brodbelt, "Streamlining bottom-up protein identification based on selective ultraviolet photodissociation (UVPD) of chromophore-tagged histidine- and tyrosine-containing peptides," Anal. Chem. **86**, 6237–6244 (2014).
[39] M. Mulcahy, J. G. McInerney, D. N. Nikogosyan, and H. Görner, "193 nm photolysis of aromatic and aliphatic dipeptides in aqueous solution: Dependence of decomposition quantum yield on the amino acid sequence," Biol. Chem. **381**, 1259 (2000).
[40] D. N. Nikogosyan and H. Gorner, "Laser-induced photodecomposition of amino acids and peptides: Extrapolation to corneal collagen," IEEE J. Sel. Top. Quantum Electron. **5**, 1107–1115 (1999).
[41] D. N. Nikogosyan and H. Görner, "Photolysis of aromatic amino acids in aqueous solution by nanosecond 248 and 193 nm laser light," J. Photochem. Photobiol., B **13**, 219–234 (1992).
[42] E. V. Khoroshilova, Y. A. Repeyev, and D. N. Nikogosyan, "UV protolysis of aromatic amino acids and related dipeptides and tripeptides," J. Photochem. Photobiol., B **7**, 159–172 (1990).
[43] D. N. Nikogosyan and H. Görner, "Towards the laser photochemistry of the cornea: Studies of the most common and highly absorbing aliphatic amino acids in collagen," J. Photochem. Photobiol., B **47**, 63–67 (1998).
[44] R. R. Hill, J. D. Coyle, D. Birch, E. Dawe, G. E. Jeffs, D. Randall, I. Stec, and T. M. Stevenson, "Photochemistry of dipeptides in aqueous solution," J. Am. Chem. Soc. **113**, 1805–1817 (1991).
[45] R. R. Hill, G. E. Jeffs, F. Banaghan, T. McNally, and A. R. Werninck, "Photo-induced electron transfer in small peptides: Glycylalanine," J. Chem. Soc., Perkin Trans. 2 **1996**(8), 1595–1599.
[46] J. Thøgersen, A. S. Chatterley, T. Weidner, and F. Jensen, "Peptide bond of aqueous dipeptides is resilient to deep ultraviolet irradiation," J. Am. Chem. Soc. **145**, 9777–9785 (2023).
[47] J. W. Preiss and R. Setlow, "Spectra of some amino acids, peptides, nucleic acids, and protein in the vacuum ultraviolet," J. Chem. Phys. **25**, 138–141 (1956).
[48] M. Buonanno, D. Welch, I. Shuryak, and D. J. Brenner, "Far-UVC light (222 nm) efficiently and safely inactivates airborne human coronaviruses," Sci. Rep. **10**, 10285 (2020).
[49] M. Buonanno, B. Ponnaiya, D. Welch, M. Stanislauskas, G. Randers-Pehrson, L. Smilenov, F. D. Lowy, D. M. Owens, and D. J. Brenner, "Germicidal efficacy and mammalian skin safety of 222-nm UV light," Radiat. Res. **187**, 493–501 (2017).
[50] M. Hessling, R. Haag, N. Sieber, and P. Vatter, "The impact of far-UVC radiation (200–230 nm) on pathogens, cells, skin, and eyes–a collection and analysis of a hundred years of data," GMS Hyg. Infect. Control **16**, Doc07 (2021).
[51] S. H. Yoon, J. H. Moon, and M. S. Kim, "Dissociation mechanisms and implication for the presence of multiple conformations for peptide ions with arginine at the C-terminus: Time-resolved photodissociation study," J. Mass Spectrom. **45**, 806–814 (2010).
[52] M. Lanzillotti and J. S. Brodbelt, "Comparison of top-down protein fragmentation induced by 213 and 193 nm UVPD," J. Am. Soc. Mass Spectrom. **34**, 279–285 (2023).
[53] D. R. Klein, D. D. Holden, and J. S. Brodbelt, "Shotgun analysis of rough-type lipopolysaccharides using ultraviolet photodissociation mass spectrometry," Anal. Chem. **88**, 1044–1051 (2016).
[54] ExciStar: Compact, High Repetition Rate Excimer Laser, Coherent, 2023.
[55] A. Theisen, C. A. Wootton, A. Haris, T. E. Morgan, Y. P. Y. Lam, M. P. Barrow, and P. B. O'Connor, "Enhancing biomolecule analysis and 2DMS experiments by implementation of (activated ion) 193 nm UVPD on a FT-ICR mass spectrometer," Anal. Chem. **94**, 15631–15638 (2022).
[56] Q. Luo, J. Ma, M. Wang, T. Lu, and X. Zhu, "All-solid-state far-UVC pulse laser at 222 nm wavelength for UVC disinfection," Chin. Opt. Lett. **21**, 011401 (2023).
[57] K. Ahlawat, R. Jangra, A. Ish, N. Jain, and R. Prakash, "A dielectric barrier discharge based low pressure narrow band far UV-C 222 nm excimer lamp and its efficiency analysis," Phys. Scr. **99**, 025018 (2024).
[58] S. Ranjan and D. D. Sasselov, "Constraints on the early terrestrial surface UV environment relevant to prebiotic chemistry," Astrobiology **17**, 169–204 (2017).
[59] S. Ranjan, C. L. Kufner, G. G. Lozano, Z. R. Todd, A. Haseki, and D. D. Sasselov, "UV transmission in natural waters on prebiotic earth," Astrobiology **22**, 242–262 (2022).
[60] R. Wolfenden, "Benchmark reaction rates, the stability of biological molecules in water, and the evolution of catalytic power in enzymes," Annu. Rev. Biochem. **80**, 645–667 (2011).
[61] G. Danger, R. Plasson, and R. Pascal, "Pathways for the formation and evolution of peptides in prebiotic environments," Chem. Soc. Rev. **41**, 5416–5429 (2012).
[62] M. Frenkel-Pinter, M. Samanta, G. Ashkenasy, and L. J. Leman, "Prebiotic peptides: Molecular hubs in the origin of life," Chem. Rev. **120**, 4707–4765 (2020).
[63] W. Taylor, E. Camilleri, D. L. Craft, G. Korza, M. R. Granados, J. Peterson, R. Szczpaniak, S. K. Weller, R. Moeller, T. Douki *et al.*, "Dna damage kills bacterial spores and cells exposed to 222-nanometer UV radiation," Appl. Environ. Microbiol. **86**, e03039 (2020).
[64] K. Narita, K. Asano, K. Naito, H. Ohashi, M. Sasaki, Y. Morimoto, T. Igarashi, and A. Nakane, "Ultraviolet C light with wavelength of 222 nm inactivates a wide spectrum of microbial pathogens," J. Hosp. Infect. **105**, 459–467 (2020).
[65] H. H. Jaffé and A. L. Miller, "The fates of electronic excitation energy," J. Chem. Educ. **43**, 469 (1966).
[66] T. Kumpulainen, B. Lang, A. Rosspeintner, and E. Vauthey, "Ultrafast elementary photochemical processes of organic molecules in liquid solution," Chem. Rev. **117**, 10826–10939 (2017).

© Author(s) 2025